



Quantum Heating of a Nonlinear Resonator Probed by a Superconducting Qubit

F. R. Ong,^{1,2} M. Boissonneault,^{3,4} F. Mallet,⁵ A. C. Doherty,⁶ A. Blais,³ D. Vion,¹ D. Esteve,¹ and P. Bertet¹

¹*Quantronics group, Service de Physique de l'État Condensé (CNRS URA 2464), IRAMIS, DSM, CEA-Saclay, 91191 Gif-sur-Yvette, France*

²*Institute for Quantum Computing, Waterloo Institute for Nanotechnology, University of Waterloo, Waterloo, Ontario, Canada N2L 3G1*

³*Département de Physique, Université de Sherbrooke, Sherbrooke, Québec, Canada J1K 2R1*

⁴*Calcul Québec, Université Laval, Québec, Québec, Canada G1V 0A6*

⁵*Laboratoire Pierre Aigrain, Ecole Normale Supérieure, CNRS (UMR 8551), Université Pierre et Marie Curie, 24, rue Lhomond, 75005 Paris, France*

⁶*Centre for Engineered Quantum Systems, School of Physics, The University of Sydney, Sydney, New South Wales 2006, Australia*
(Received 5 October 2012; published 22 January 2013)

We measure the quantum fluctuations of a pumped nonlinear resonator using a superconducting artificial atom as an *in situ* probe. The qubit excitation spectrum gives access to the frequency and amount of excitation of the intracavity field fluctuations, from which we infer its effective temperature. These quantities are found to be in agreement with theoretical predictions; in particular, we experimentally observe the phenomenon of quantum heating.

DOI: [10.1103/PhysRevLett.110.047001](https://doi.org/10.1103/PhysRevLett.110.047001)

PACS numbers: 85.25.Cp, 03.67.Lx

A resonator in which a nonlinear medium is inserted has rich dynamics when it is driven by an external pump field [1]. In the case of a Kerr medium, the field amplitude inside such a Kerr nonlinear resonator (KNR) switches from a low to a high value when the pump reaches a certain threshold, a phenomenon known as bistability in optics [2] and bifurcation in the microwave domain [3]. This hysteretic transition between two dynamical states is a stochastic process triggered by fluctuations around the steady-state pumped oscillations. Given the potential applications for low-power all-optical logical elements such as switches and transistors [4], a quantitative understanding of these fluctuations governing the sharpness of the transition, and therefore the device performance, is highly desirable [5,6]. In a KNR operated in the quantum regime [7], field fluctuations are mainly due to spontaneous parametric down-conversion (SPDC) [8–10] of pairs of photons at the pump frequency ω_p into pairs of photons, one at the characteristic pumped-KNR frequency $\tilde{\omega}_c$ and the other at the complementary idler frequency $\omega_i = 2\omega_p - \tilde{\omega}_c$. The mode at $\tilde{\omega}_c$ therefore acquires a nonzero photon population, with a statistics that can be shown theoretically to be thermal. Its effective temperature depends on the pump frequency and power and is nonzero even when the electromagnetic bath to which it is coupled is at zero temperature, a central theoretical prediction known as quantum heating that remains to be tested [7,11–13].

Up to now, experiments in the optical or microwave domains have only measured the spectrum of the field radiated by a pumped KNR [14]. In this work, we access the intraresonator field fluctuations by inserting a two-level system inside the KNR and using it as an absolute spectrometer and thermometer, as illustrated in Fig. 1(a).

The experiment is performed in the microwave domain at millikelvin temperatures using superconducting Josephson circuits. The KNR is a coplanar waveguide (CPW) resonator with an embedded Josephson junction [15,16], and the two-level system is a transmon qubit [17] [see Fig. 1(b)]. By measuring the qubit absorption spectrum while pumping the KNR, we obtain a quantitative agreement with the average number of excitations predicted by the theory of quantum heating [11–13].

We start with a rapid summary of the relevant theoretical results regarding the quantum fluctuations of a KNR—more details can be found in Refs. [5,7,11,13,18–20]. The KNR, driven by a field of power P_p and frequency ω_p , is modeled in the frame rotating at ω_p by the Hamiltonian $\bar{H}_c/\hbar = \Delta_p \bar{a}^\dagger \bar{a} + \frac{K}{2} \bar{a}^{\dagger 2} \bar{a}^2 + \frac{K'}{3} \bar{a}^{\dagger 3} \bar{a}^3 + (i\epsilon_p \bar{a}^\dagger + \text{H.c.})$ with $\Delta_p = \omega_c - \omega_p$, ω_c the KNR resonance frequency in its linear regime, \bar{a} and \bar{a}^\dagger the KNR field annihilation and creation operators, $\epsilon_p = \sqrt{\kappa P_p/\hbar\omega_p}$ the driving amplitude, κ the resonator energy damping rate, and K and K' the Kerr nonlinear constants derived from circuit parameters [16,21]. The steady-state solution for the dimensionless cavity field amplitude α is obtained from the corresponding master equation, yielding $(\Omega \frac{\kappa}{2} + K|\alpha|^2 + K'|\alpha|^4 - i\frac{\kappa}{2})\alpha = -i\epsilon_p$, with $\Omega = 2Q\Delta_p/\omega_c$ the reduced pump frequency [18,20] and $Q = \omega_c/\kappa$ the resonator quality factor. For $\Omega > \sqrt{3}$ and P_p larger than the critical power $P_c = \frac{\kappa^2}{3\sqrt{3}|K|}\hbar\omega_p$, this equation admits two stable solutions $\alpha_{L,H}$ corresponding to metastable dynamical states L and H of low and high amplitudes, respectively [18]. In this bistable and hysteretic regime, the transition from L to H occurs abruptly when ramping up the pump power at the bifurcation threshold $P_+(\Omega)$. The corresponding stability diagram is shown in Fig. 1(c).

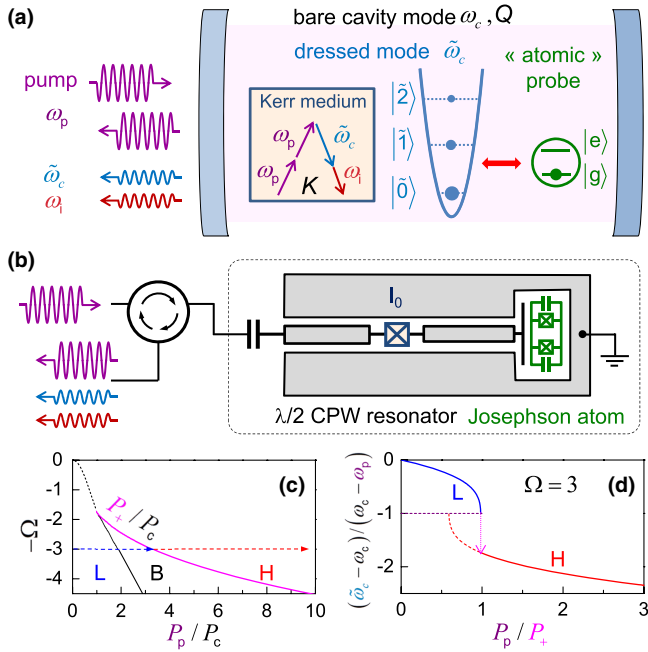


FIG. 1 (color online). (a) Optical analogue of the experiment: A Fabry-Pérot cavity with resonance frequency ω_c , quality factor Q , and Kerr nonlinearity K is pumped at frequency ω_p . Photons are produced at the cavity dressed mode frequency $\tilde{\omega}_c$ and at the idler frequency ω_i by SPDC of pump photon pairs. An *in situ* atomic probe is used as an absolute spectrometer and thermometer to characterize this quantum heating of the dressed mode. (b) Actual experiment: The cavity is a microwave superconducting $\lambda/2$ coplanar waveguide resonator, the Kerr medium a Josephson junction, and the probe a transmon artificial atom. (c) Stability diagram of the resonator in the pump power P_p and frequency ω_p plane (in reduced units, see the text): L , H , and B denote regions where the amplitude of the driven oscillations is low, high, and bistable, respectively. P_+ is the pump power at which the field switches from L to H when P_p is increased. (d) Dressed mode frequency $\tilde{\omega}_c$ when increasing P_p at $\Omega = 3$ [along the arrows of (c)].

We consider here the quantum fluctuations of the intracavity field around its steady-state value α , in the regime where they are too weak to induce switching to the other dynamical state within the experiment duration. This justifies linearizing \tilde{H}_c around α , by writing $\tilde{a} = \alpha + a$ and keeping only terms quadratic in a . Following Ref. [20], this linearized Hamiltonian can be diagonalized by introducing a new operator $\tilde{a} = \mu a + \nu a^\dagger$ and rewritten as $\tilde{H}_l = \tilde{\Delta}_p \tilde{a}^\dagger \tilde{a}$ with $\tilde{\Delta}_p = \text{sign}(A)\sqrt{B}$, $A = \Delta_p + 2K|\alpha|^2 + 3K'|\alpha|^4$, and $B = A^2 - (K + 2K'|\alpha|^2)^2|\alpha|^4$. In the laboratory frame, intracavity field fluctuations are thus described as excitations of a harmonic dressed mode of resonance frequency $\tilde{\omega}_c = \omega_p + \tilde{\Delta}_p$ that depends on the pump amplitude and frequency [22]. We note the eigenstates of this effective oscillator $|\tilde{n}\rangle = (\tilde{a}^\dagger)^n |\tilde{0}\rangle / \sqrt{n!}$. As shown in Fig. 1(d) for the case where $K, K' < 0$ and $\Delta_p > 0$ as in our experiment, the dressed

frequency $\tilde{\omega}_c$ is equal to ω_c at low pump power, then decreases when P_p is increased, reaching ω_p when $P_p = P_+$, which causes the field to jump to its high amplitude value and $\tilde{\omega}_c$ correspondingly to jump well below ω_p . The dressed mode is damped at the same rate κ as the KNR but toward an equilibrium steady state at a finite effective temperature T_{eff} corresponding to a mean number of excitations $\langle \tilde{n} \rangle$ equal to $|\nu|^2$, even if the bath physical temperature is zero [20]. Physically, this thermal population is caused by SPDC of pairs of pump photons at ω_p into correlated photons at frequencies $\tilde{\omega}_c$ and $\omega_i = 2\omega_p - \tilde{\omega}_c$, emitted in the dressed mode and in the measuring line, respectively; the apparent thermal character of the intracavity field is obtained when neglecting the correlations between the $\tilde{\omega}_c$ and the ω_i photons. Note that this analysis is only valid if $B > 0$, a condition verified sufficiently far from the bifurcation threshold, as is the case here.

In our experimental test of these predictions, the KNR is a superconducting coplanar waveguide resonator including a Josephson junction with frequency $\omega_c/2\pi = 6.4535$ GHz, Kerr constants $K/2\pi = -625$ kHz and $K'/2\pi = -1.25$ kHz, and damping rate $\kappa/2\pi = 10$ MHz [see Fig. 1(d)] [16]. It is capacitively coupled with strength $g/2\pi = 44$ MHz to a superconducting qubit of the transmon type with frequency $\omega_{\text{ge}}/2\pi = 5.718$ GHz. Because of the large qubit-resonator detuning, their interaction can be described in the so-called dispersive limit [23]. The resonator and the qubit can be driven by microwave pulses applied to the resonator input. The qubit can be readout in a single shot by driving the resonator close to its bifurcation threshold $P_+(\Omega)$ in order to map the qubit states $|g\rangle$ and $|e\rangle$ to the L and H states, respectively [24].

A first method to investigate the field fluctuations of the pumped KNR is to measure the spectrum of the field radiated into the measurement line, as reported recently [14,25]. Using the setup of Fig. 2(a) [26], we perform homodyne detection of the field quadratures at ω_p and compute their total power spectrum $S(\Delta\omega)$, which is proportional to the sum of the spectral power density at $\omega_p + \Delta\omega$ and at $\omega_p - \Delta\omega$. The data show a peak at a P_p -dependent frequency [see Figs. 2(b) and 2(c)]. All the sample parameters being known from earlier measurements [16], the theoretical $\tilde{\Delta}_p(P_p)$ curve can be computed without adjustable parameters and is shown in Fig. 2(c). Except for avoided crossings at $\tilde{\Delta}_p/2\pi \approx 40$ and 70 MHz of unknown origin, the agreement is quantitative. The observed peak thus indeed results from noise generated by the pumped KNR at $\omega_p + \tilde{\Delta}_p = \tilde{\omega}_c$ and $\omega_p - \tilde{\Delta}_p = \omega_i$. However, these measurements are unable to determine the effective temperature of the mode $\tilde{\omega}_c$ from which the measured photons are leaking, which is the key quantity of the theory discussed above.

A two-level system such as the transmon qubit is an ideal *in situ* probe of quantum heating because it acts as an

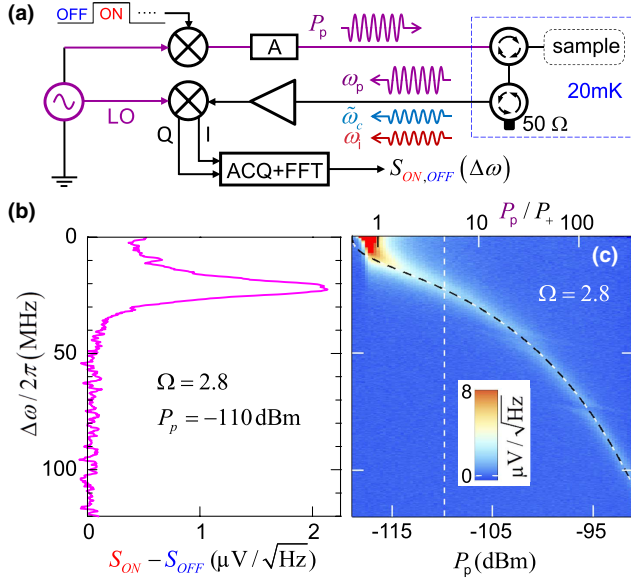


FIG. 2 (color online). Measurement of the field radiated by the KNR pumped at $\Omega = 2.8$ ($\omega_p/2\pi = 6.4395$ GHz). (a) Experimental setup: The pump tone, sent through a line with attenuators (A), is switched on and off every 2.5 ms; the reflected and radiated signals are amplified and mixed down at ω_p , yielding two quadratures $I(t)$ and $Q(t)$ that are digitized by an acquisition card (ACQ) and Fourier transformed (FFT); the total voltage spectral densities $S_{ON,OFF}(\Delta\omega = |\omega - \omega_p|)$ for the two pump states are then computed. (b) Radiated noise spectrum $S_{ON} - S_{OFF}$ for $P_p = -110$ dBm. (c) Radiated noise spectrum as a function of P_p . The dashed curve is the calculated $\Delta_p = \tilde{\omega}_p - \omega_p(P_p)$. The vertical dotted line indicates the cut shown in (b).

absolute spectrometer and thermometer for a given quantum noise source [27,28]. We infer the temperature of the $\tilde{\omega}_c$ mode while keeping the qubit and KNR far detuned by using a method called sideband spectroscopy, which is routinely used in ion-trapping experiments [29,30] and has also been applied recently to mechanical oscillators [31]. Indeed, starting from the system in state $|g, \tilde{n}\rangle$ it is possible to drive a transition to $|e, \tilde{n} + 1\rangle$ by irradiating the qubit at frequency $\omega_{ge} + \tilde{\omega}_c$ (the so-called Stokes sideband) or to $|e, \tilde{n} - 1\rangle$, provided $\tilde{n} > 0$ by irradiating the qubit at $|\omega_{ge} - \tilde{\omega}_c|$ (the so-called anti-Stokes sideband) [32–34]. In the case of a transmon qubit, these transitions need to be driven with two photons of arbitrary frequency, provided their sum (difference) satisfies the Stokes (anti-Stokes) sideband resonance condition [35]. Given the sideband transition matrix element dependence on \tilde{n} , one can show that the average photon number $\langle \tilde{n} \rangle = 1/[\exp(\hbar\tilde{\omega}_p/kT_{\text{eff}}) - 1]$ is equal to $r/(1 - r)$ with $r \in [0, 1]$, the anti-Stokes-to-Stokes sideband peak amplitude ratio [30]. Measurement of the qubit absorption spectrum, yielding r , therefore corresponds to a measurement of T_{eff} .

Sideband spectroscopy is performed using the setup shown in Fig. 3(a). Once a steady-state pump field is established in the resonator, a spectroscopy pulse is applied to the qubit at fixed power P_q and varying frequency ω_q . The pump tone provides one of the two photons needed to drive the sideband transitions, and the spectroscopy tone provides the second photon whenever ω_q matches the Stokes [anti-Stokes] sideband resonance condition $\omega_q + \omega_p = \omega_{ge} + \tilde{\omega}_c(P_p)$ [$\omega_p - \omega_q = \tilde{\omega}_c(P_p) - \omega_{ge}$]. The experimental sequence ends by reading out the qubit state 200 ns after both pulses are switched off, long enough

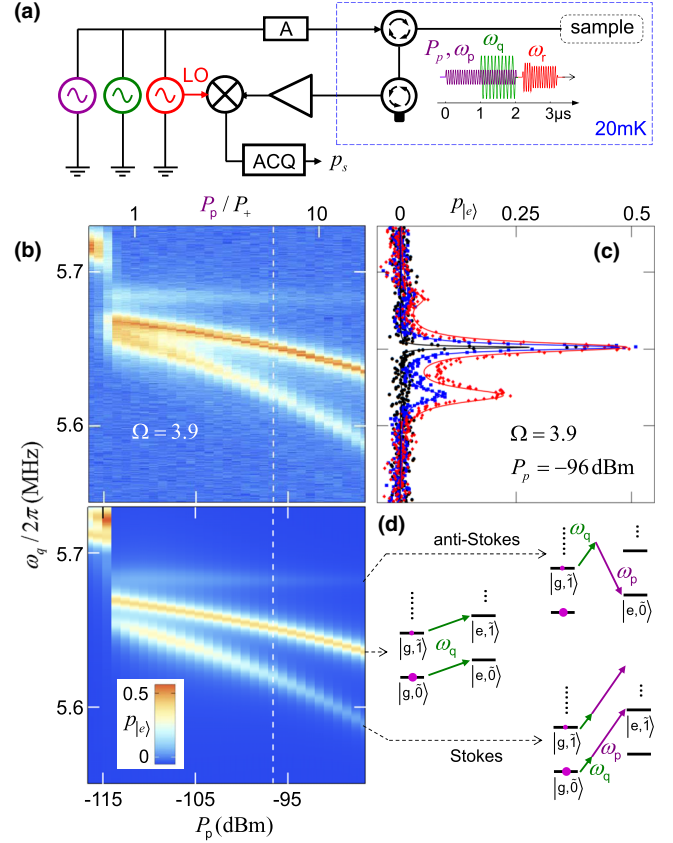


FIG. 3 (color online). Sideband spectroscopy of the qubit while pumping the resonator with varying power P_p at $\Omega = 3.9$ ($\omega_p/2\pi = 6.434$ GHz). (a) Experimental setup: A spectroscopic pulse is applied at ω_q with power P_q during the pumping; the pump and spectroscopy tones are then switched off and the qubit is measured using a third pulse at ω_r with a power close to the bifurcation threshold P_+ . The measured phase of the reflected pulse yields the qubit state, and repeating the sequence yields the qubit excited state probability $p_{|e\rangle}$. (b) Measured (top) and calculated (bottom) 2D plots showing the $p_{|e\rangle}(\omega_q)$ spectra as a function of P_p (bottom axis), also expressed in units of the bifurcation threshold P_+ (top axis). (c) Experimental (dots) and analytical (lines) spectra at a power $P_p = -96$ dBm [dashed lines in (b)] for powers $P_q = -131, -120,$ and -115 dBm (from left to right). (d) Energy diagrams showing the transitions involved in the red sideband peak (Stokes), the central peak, and the blue sideband (anti-Stokes).

for the KNR field to decay but shorter than the qubit relaxation time $T_1 \approx 700$ ns [16]; repeating this sequence $\approx 10^4$ times yields the qubit excited state probability $p_{|e\rangle}$.

Typical data are shown in Fig. 3(c) at $\Omega = 3.9$ and $P_p = -96$ dBm such that the KNR is in the high oscillation amplitude state H . At low spectroscopy power P_q , only one Lorentzian peak is visible, corresponding to the qubit frequency ac-Stark shifted by the steady-state intraresonator field with mean photon number $\langle n_H \rangle = |\alpha_H|^2$ at ω_p [16,36]. Increasing the spectroscopy power, we observe the appearance of two satellite peaks around ω_{ge} , with a separation of 31 MHz that closely matches the value of $\hat{\Delta}_p = \omega_p - \tilde{\omega}_c(P_p)$, already known without any adjustable parameters as explained above. When P_p is varied, this separation also quantitatively varies as expected from the $\tilde{\omega}_c$ dependence on P_p , as shown in Fig. 3(b). This establishes that the satellite peaks are indeed the sideband transitions. The anti-Stokes sideband being observed and of smaller amplitude than the Stokes sideband indicates that the temperature of the dressed mode is nonzero, as discussed in more detail below.

To be more quantitative, we have performed a detailed theoretical analysis [20] of the coupled qubit-KNR system that will be presented elsewhere [37] and that yields analytical approximate expressions for the qubit sideband spectrum. The predictions, calculated with a global attenuation factor on the spectroscopy power P_q as the only adjustable parameter, are also shown in Figs. 3(b) and 3(c) for different P_q ; they agree quantitatively with the data. Since these calculations are done at zero bath temperature, this is a first clear indication that the population of the mode at $\tilde{\omega}_c$ is only due to SPDC and is therefore of quantum origin.

Assuming that the field in the dressed mode $\tilde{\omega}_c$ has the statistics of a thermal field as predicted theoretically, we now extract an experimental occupation number of the dressed mode from the relative height of the two sideband peaks and translate it into an effective temperature T_{eff} . For this, each spectrum of Fig. 3(b) is fitted to a sum of three Lorentzians of adjustable frequency, width, and height, yielding the ratios r of the anti-Stokes-to-Stokes sideband height. Figure 4 shows the comparison between the experimental occupation number $r/(1-r)$ and $\langle \tilde{n} \rangle$ calculated without any adjustable parameter. The data agree fairly well with the prediction, demonstrating that the average photon number in the dressed mode is indeed $|\nu|^2$ as predicted by theory (see Chap. 7 in Ref. [1]). More precisely, we estimate that the residual thermal field at $\tilde{\omega}_c$ cannot be responsible for more than 20% of the observed signal. Our data show that the dressed mode occupation number and temperature are maximum near the bifurcation threshold P_+ and decrease with increasing pumping power and occupation number $\langle n_H \rangle$ at ω_p . This constitutes additional evidence that the measured thermal field is not due to a trivial heating caused by the microwave

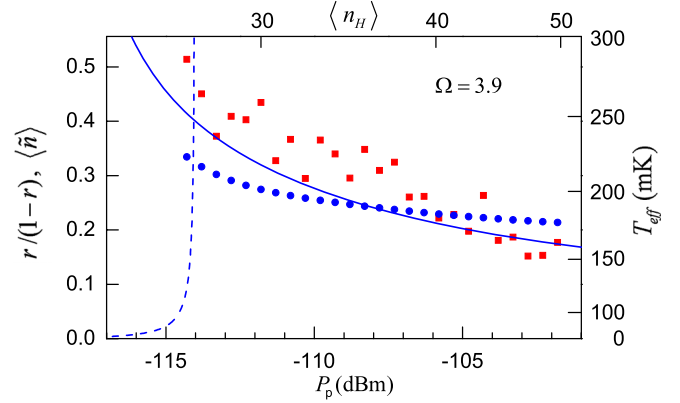


FIG. 4 (color online). Quantum heating of the pumped resonator mode $\tilde{\omega}_c$ above bifurcation: Quantity $r/(1-r)$ with r being the ratio of blue to red sideband peak heights deduced from the experimental (squares) and theoretical (dots) qubit spectra of Fig. 3(b), as a function of the pump power P_p (bottom axis). The calculated average number $\langle n_H \rangle$ of photons in the pump mode is indicated on the top axis. In a simple theoretical picture, $r/(1-r)$ is the average photon number $\langle \tilde{n} \rangle$ in the $\tilde{\omega}_c$ mode, shown here as a dashed and a solid line for the L and H resonator states, respectively. The corresponding effective temperature T_{eff} is indicated on the right axis.

pulses. We also stress that these results do not rely on any calibration of the measurement lines or temperature. Finally, we also show in Fig. 4 the quantity $r/(1-r)$ derived from the analytical expression that yielded the theoretical spectra shown in Fig. 3: It is in agreement with both the experimental data and the simple formula for the KNR effective temperature. Additional data can be found in the Supplemental Material [20] taken on another sample with different parameters, with which similar results have been obtained.

In conclusion, we have probed the quantum fluctuations of a pumped nonlinear resonator with an embedded superconducting qubit, bringing experimental evidence of quantum heating. Future directions include establishing the link between quantum heating and the switching rates at the bistability threshold [11] and testing the thermal character of the dressed resonator mode by performing its quantum state tomography with the qubit [38]. In general, our experiments demonstrate that detailed and quantitative tests of all theoretical predictions regarding nonlinear resonators in the quantum regime are enabled by the progress of superconducting circuits.

We acknowledge useful discussions with M. Dykman and within the Quantronics Group, as well as technical support from P. Sénat, P.-F. Orfila, T. David, and J.-C. Tack. We acknowledge support from NSERC, the Alfred P. Sloan Foundation, CIFAR, the European project SOLID, the C’Nano project QUANTROCRYO, and the Australian Research Council via the Centre of Excellence in Engineered Quantum Systems (EQuS), Project No. CE110001013.

- [1] *Fluctuating Nonlinear Oscillators*, edited by M. Dykman (Oxford University Press, Oxford, England, 2012).
- [2] L. Lugiato, *Prog. Opt.* **21**, 69 (1984).
- [3] I. Siddiqi, R. Vijay, F. Pierre, C. M. Wilson, L. Frunzio, M. Metcalfe, C. Rigetti, R. J. Schoelkopf, M. H. Devoret, D. Vion, and D. Esteve, *Phys. Rev. Lett.* **94**, 027005 (2005).
- [4] K. Nozaki, T. Tanabe, A. Shinya, S. Matsuo, T. Sato, H. Taniyama, and M. Notomi, *Nat. Photonics* **4**, 477 (2010).
- [5] M. Dykman and V. Smelyansky, *Zh. Eksp. Teor. Fiz.* **94**, 61 (1988) [*Sov. Phys. JETP* **67**, 1769 (1988)].
- [6] R. Vijay, M. H. Devoret, and I. Siddiqi, *Rev. Sci. Instrum.* **80**, 111101 (2009).
- [7] P. D. Drummond and D. F. Walls, *J. Phys. A* **13**, 725 (1980).
- [8] S. E. Harris, M. K. Oshman, and R. L. Byer, *Phys. Rev. Lett.* **18**, 732 (1967).
- [9] D. C. Burnham and D. L. Weinberg, *Phys. Rev. Lett.* **25**, 84 (1970).
- [10] D. Bouwmeester, J. Pan, K. Mattle, M. Eibl, H. Weinfurter, and A. Zeilinger, *Nature (London)* **390**, 575 (1997).
- [11] M. Marthaler and M. I. Dykman, *Phys. Rev. A* **73**, 042108 (2006).
- [12] M. I. Dykman, M. Marthaler, and V. Peano, *Phys. Rev. A* **83**, 052115 (2011).
- [13] S. Andre, L. Guo, V. Peano, M. Marthaler, and G. Schoen, *Phys. Rev. A* **85**, 053825 (2012).
- [14] P. Lahteenmaki, G. S. Paraoanu, J. Hassel, and P. J. Hakonen, [arXiv:1111.5608](https://arxiv.org/abs/1111.5608).
- [15] E. Boaknin, V. E. Manucharyan, S. Fissette, M. Metcalfe, L. Frunzio, R. Vijay, I. Siddiqi, A. Wallraff, R. J. Schoelkopf, and M. Devoret, [arXiv:cond-mat/0702445](https://arxiv.org/abs/cond-mat/0702445).
- [16] F. R. Ong, M. Boissonneault, F. Mallet, A. Palacios-Laloy, A. Dewes, A. C. Doherty, A. Blais, P. Bertet, D. Vion, and D. Esteve, *Phys. Rev. Lett.* **106**, 167002 (2011).
- [17] J. Koch, T. M. Yu, J. Gambetta, A. A. Houck, D. I. Schuster, J. Majer, A. Blais, M. H. Devoret, S. M. Girvin, and R. J. Schoelkopf, *Phys. Rev. A* **76**, 042319 (2007).
- [18] B. Yurke and E. Buks, *J. Lightwave Technol.* **24**, 5054 (2006).
- [19] C. Laffamme and A. A. Clerk, *Phys. Rev. A* **83**, 033803 (2011).
- [20] See Supplemental Material at <http://link.aps.org/supplemental/10.1103/PhysRevLett.110.047001> for a self-standing theory of quantum heating, as well as complementary experimental data.
- [21] In order to obtain quantitative understanding of our experiments, we need to include not only the standard Kerr nonlinearity term $\frac{K}{2}\bar{a}^{+2}\bar{a}^2$ but also the next order nonlinearity $\frac{K'}{3}\bar{a}^{+3}\bar{a}^3$. This term does not change the physics described in this article; hence, we still speak of the Kerr nonlinear resonator by convenience.
- [22] Note that the separation between the energy levels of the effective resonator in the rotating frame $\hbar\tilde{\Delta}_p$ is called quasienergy by several authors.
- [23] A. Blais, R.-S. Huang, A. Wallraff, S. M. Girvin, and R. J. Schoelkopf, *Phys. Rev. A* **69**, 062320 (2004).
- [24] F. Mallet, F. Ong, A. Palacios-Laloy, F. Nguyen, P. Bertet, D. Vion, and D. Esteve, *Nat. Phys.* **5**, 791 (2009).
- [25] C. M. Wilson, G. Johansson, A. Pourkabirian, M. Simoen, J. R. Johansson, T. Duty, F. Nori, and P. Delsing, *Nature (London)* **479**, 376 (2011).
- [26] A. Palacios-Laloy, F. Mallet, F. Nguyen, P. Bertet, D. Vion, D. Esteve, and A. N. Korotkov, *Nat. Phys.* **6**, 442 (2010).
- [27] R. Schoelkopf, A. Clerk, S. Girvin, K. Lehnert, and M. Devoret, in *Proceedings of the NATO Advanced Research Workshop on Quantum Noise in Mesoscopic Physics, Delft, the Netherlands, 2002*, Nato Science Series, Series II: Mathematics, Physics and Chemistry, Vol. 97, edited by Y. Nazarov (Kluwer, Dordrecht, 2003), p. 175.
- [28] I. Serban, M. I. Dykman, and F. K. Wilhelm, *Phys. Rev. A* **81**, 022305 (2010).
- [29] F. Diedrich, J. C. Bergquist, W. M. Itano, and D. J. Wineland, *Phys. Rev. Lett.* **62**, 403 (1989).
- [30] Q. A. Turchette, D. Kielpinski, B. E. King, D. Leibfried, D. M. Meekhof, C. J. Myatt, M. A. Rowe, C. A. Sackett, C. S. Wood, W. M. Itano, C. Monroe, and D. J. Wineland, *Phys. Rev. A* **61**, 063418 (2000).
- [31] A. H. Safavi-Naeini, J. Chan, J. T. Hill, T. P. M. Alegre, A. Krause, and O. Painter, *Phys. Rev. Lett.* **108**, 033602 (2012).
- [32] I. Chiorescu, P. Bertet, K. Semba, Y. Nakamura, C. J. P. M. Harmans, and J. E. Mooij, *Nature (London)* **431**, 159 (2004).
- [33] A. Wallraff, D. I. Schuster, A. Blais, J. M. Gambetta, J. Schreier, L. Frunzio, M. H. Devoret, S. M. Girvin, and R. J. Schoelkopf, *Phys. Rev. Lett.* **99**, 050501 (2007).
- [34] P. J. Leek, S. Filipp, P. Maurer, M. Baur, R. Bianchetti, J. M. Fink, M. Göppl, L. Steffen, and A. Wallraff, *Phys. Rev. B* **79**, 180511 (2009).
- [35] A. Blais, J. Gambetta, A. Wallraff, D. I. Schuster, S. M. Girvin, M. H. Devoret, and R. J. Schoelkopf, *Phys. Rev. A* **75**, 032329 (2007).
- [36] M. Boissonneault, A. C. Doherty, F. R. Ong, P. Bertet, D. Vion, D. Esteve, and A. Blais, *Phys. Rev. A* **85**, 022305 (2012).
- [37] M. Boissonneault, A. C. Doherty, F. R. Ong, P. Bertet, D. Vion, D. Esteve, and A. Blais (to be published).
- [38] M. Hofheinz, H. Wang, M. Ansmann, R. C. Bialczak, E. Lucero, M. Neeley, A. D. O'Connell, D. Sank, J. Wenner, J. M. Martinis, and A. N. Cleland, *Nature (London)* **459**, 546 (2009).